

**MASTER COPY:** PLEASE KEEP THIS "MEMORANDUM OF TRANSMITTAL" BLANK FOR REPRODUCTION PURPOSES. WHEN REPORTS ARE GENERATED UNDER THE ARO SPONSORSHIP, FORWARD A COMPLETED COPY OF THIS FORM WITH EACH REPORT SHIPMENT TO THE ARO. THIS WILL ASSURE PROPER IDENTIFICATION. NOT TO BE USED FOR INTERIM PROGRESS REPORTS; SEE PAGE 2 FOR INTERIM PROGRESS REPORT INSTRUCTIONS.

**MEMORANDUM OF TRANSMITTAL**

U.S. Army Research Office  
ATTN: AMSRL-RO-BI (TR)  
P.O. Box 12211  
Research Triangle Park, NC 27709-2211

Reprint (Orig + 2 copies)

Technical Report (Orig + 2 copies)

Manuscript (1 copy)

Final Progress Report (Orig + 2 copies)

Related Materials, Abstracts, Theses (1 copy)

CONTRACT/GRANT NUMBER:

REPORT TITLE:

is forwarded for your information.

SUBMITTED FOR PUBLICATION TO (applicable only if report is manuscript):

Sincerely,

# REPORT DOCUMENTATION PAGE

Form Approved  
OMB NO. 0704-0188

Public Reporting burden for this collection of information is estimated to average 1 hour per response, including the time for reviewing instructions, searching existing data sources, gathering and maintaining the data needed, and completing and reviewing the collection of information. Send comment regarding this burden estimates or any other aspect of this collection of information, including suggestions for reducing this burden, to Washington Headquarters Services, Directorate for information Operations and Reports, 1215 Jefferson Davis Highway, Suite 1204, Arlington, VA 22202-4302, and to the Office of Management and Budget, Paperwork Reduction Project (0704-0188,) Washington, DC 20503.

1. AGENCY USE ONLY ( Leave Blank)		2. REPORT DATE		3. REPORT TYPE AND DATES COVERED	
4. TITLE AND SUBTITLE				5. FUNDING NUMBERS	
6. AUTHOR(S)					
7. PERFORMING ORGANIZATION NAME(S) AND ADDRESS(ES)				8. PERFORMING ORGANIZATION REPORT NUMBER	
9. SPONSORING / MONITORING AGENCY NAME(S) AND ADDRESS(ES)  U. S. Army Research Office P.O. Box 12211 Research Triangle Park, NC 27709-2211				10. SPONSORING / MONITORING AGENCY REPORT NUMBER	
11. SUPPLEMENTARY NOTES The views, opinions and/or findings contained in this report are those of the author(s) and should not be construed as an official Department of the Army position, policy or decision, unless so designated by other documentation.					
12 a. DISTRIBUTION / AVAILABILITY STATEMENT  Approved for public release; distribution unlimited.				12 b. DISTRIBUTION CODE	
13. ABSTRACT (Maximum 200 words)					
14. SUBJECT TERMS				15. NUMBER OF PAGES	
				16. PRICE CODE	
17. SECURITY CLASSIFICATION OR REPORT <b>UNCLASSIFIED</b>		18. SECURITY CLASSIFICATION ON THIS PAGE <b>UNCLASSIFIED</b>		19. SECURITY CLASSIFICATION OF ABSTRACT <b>UNCLASSIFIED</b>	
				20. LIMITATION OF ABSTRACT <b>UL</b>	

NSN 7540-01-280-5500

Standard Form 298 (Rev.2-89)  
Prescribed by ANSI Std. 239-18  
298-102

Enclosure 1

# Information Efficiency of *Ad Hoc* Networks with FH-MIMO Transceivers

Kostas Stamatiou, John G. Proakis and James R. Zeidler

Department of Electrical & Computer Engineering

University of California San Diego, La Jolla, CA 92093-0407

Email: kostas@ucsd.edu, jproakis@cw.cw.ucsd.edu, zeidler@ucsd.edu

**Abstract**—We consider an *ad hoc* network where frequency hopping (FH) and coding are employed in order to mitigate multiple-access interference. In contrast to previous work, in our model hopping takes place at the symbol level. As a result, different interference levels are encountered across a codeword/packet, creating *interference diversity* which is exploited through coding. Moreover, the nodes are equipped with multiple antennas which can be used for further error protection or increase of the transmission rate through space-time block coding or spatial multiplexing, respectively. Assuming an infinite network of terminals, modelled as a Poisson random field, the performance is evaluated in terms of the product (spectral efficiency)  $\times$  (distance), often referred to as *information efficiency*. With a cross-layer design perspective in mind, results are presented for various combinations of routing strategies, MIMO techniques and code diversity orders.

## I. INTRODUCTION

In a multi-hop packet radio or *ad hoc* network, the larger the transmission distance, the more progress a packet makes towards its final destination. However, the amount of interference to the other terminals is also increased. This is a key trade-off in the resulting network throughput, first analyzed in [1] and further refined in [2].

The interference model used in the aforementioned work assumed that at most one successful transmission at a time can occur in a given region. In [3], the authors developed a more realistic interference model, by determining the statistics of the total interference power generated by all active transmitters in the network and using these to compute the packet success probability. More recent work that elaborated on this model, considering among other things the effects of frequency hopping, Reed-Solomon or Turbo coding, adaptive modulation and routing, includes [4]–[6]. In [4] specifically, a reasonable performance measure termed *information efficiency* was introduced to quantify the amount of information (*bits/Hz*) that can successfully be transmitted over a certain distance in the network, times that distance. Maximizing the information efficiency was then used to determine optimum network parameters such as the transmission range.

In this paper, we embark on a similar theme. Each transmitter (TX) and receiver (RX) pair communicate over a hopping pattern and power control at the TX compensates

for path loss and shadowing. This is a simple power control policy, also considered in [7]. In contrast to previous work and similarly to the recently submitted [8], each symbol in a packet/codeword is transmitted over a different frequency, thus different interference levels are encountered across the codeword. Convolutional coding is employed to harness the available interference diversity.

In addition, each node is equipped with multiple antennas. Assuming that the fading matrix is known at the RX, these can either be used for space-time block coding (STBC) or spatial multiplexing (SM), e.g. by zero-forcing (ZF), to provide further error protection or to increase the data rate, respectively. We address the question under what transmission range each multiple-input multiple-output (MIMO) technique results in larger information efficiency. The answer depends on the degree of error protection provided by the code, as expressed by the minimum Hamming distance, but also on the routing strategy. Similarly to [2], two routing strategies are considered; to the nearest and the furthest neighbor within the transmission range and along the desired direction (Nearest with Forward Progress, NFP and Most Forward Progress, MFP, respectively). For comparison purposes, results are also provided for a system without coding.

The rest of the paper is organized as follows. We describe our system model in section II. The performance analysis is carried out in section III and the information efficiency defined and evaluated in section IV. Numerical results are provided in section V and our conclusions presented in section VI.

## II. SYSTEM MODEL

### A. Network

Our model follows [3]–[6] closely. The network is a Poisson random field in the plane with density  $\lambda$ , where each node knows the location of all other nodes. The packet traffic is uniform, i.e. a node can select any other node as a final destination of its packets with equal probability and there are always packets to be transmitted in the nodes' queues. Regarding how the network topology changes with time, it is reasonable to suppose that, in a practical scenario, the node locations remain constant over several packet intervals.

Time is slotted at the packet level and we assume all nodes adhere to this common clock. A node transmits at the beginning of the slot with probability  $p$  and receives with

This work was supported by the Ericsson Grant 02-10109, UC Discovery Grant com04-10173 and MURI Grant W911NF-04-1-0224.

probability  $1 - p$ . If a node is in TX mode, it randomly selects a final destination and proceeds to transmit a packet to a RX within its transmission range, which is a disc of radius  $R_0$ . The selection of the RX is performed according to two routing strategies: NFP or MFP, where the closest or furthest RX to the desired direction is selected, respectively.

In the event that more than one TXs want to communicate with the same RX, the conflict is resolved arbitrarily. Assuming that a TX can choose between  $k$  potential NFP or MFP neighbors to transmit to (each corresponding to a different final destination), there are  $k$  potential TXs to any RX and letting  $k \rightarrow \infty$ , the probability that a TX-RX pair is formed is equal to  $\tau(p) = (1 - p)(1 - e^{-p})$ , termed as “the tendency to pair-up” in [3]. Note that  $\tau(p)$  is not based on a specific MAC protocol, which is beyond the scope of this paper.

### B. Physical Layer

The channel between each TX-RX pair comprises fading, path-loss with distance  $r$ , according to  $r^{-b}$ , and log-normal shadowing with variance  $\sigma_s^2$ . The TX compensates for path-loss and shadowing with power control (PC). It is assumed that the average (with respect to the fading) received signal-to-noise ratio is sufficiently large, such that interference from concurrent transmissions is the only cause of errors in communication. Each packet slot is divided into symbol slots of duration  $T$  and there are  $M$  frequencies available for hopping during the transmission of the packet.

The TX and RX block diagrams are shown in fig.1. The information bits of each packet are encoded, interleaved and Gray-mapped to complex symbols from a  $2^l$ -PSK or  $2^l$ -QAM constellation. In the STBC mode, a group of  $P$  complex symbols is encoded into the  $M_T \times P$  matrix  $\mathbf{X}$ , where  $M_T$  is the number of antennas and  $P \geq M_T$ . Each column of  $\mathbf{X}$  is transmitted over a symbol slot and over the same frequency. When all the columns of  $\mathbf{X}$  are transmitted, a different frequency is selected. It is assumed that the fading matrix remains constant during the  $P$  slots and changes independently at the new frequency. The received matrix  $\mathbf{Y}$  at a given frequency is expressed as

$$\mathbf{Y} = \mathbf{H}\mathbf{X} + \sum_n \alpha_n \sqrt{P_n} \mathbf{H}_n \mathbf{X}_n \quad (1)$$

where  $\mathbf{H}$  is the fading matrix between the TX and the RX with independent entries  $h_{ij} \sim \mathcal{CN}(0, 1)$ ;  $\alpha_n$  is one (zero) with probability  $p/M$  ( $1 - p/M$ ) depending on whether node  $n$  is active and occupying the same frequency or not;  $\mathbf{H}_n$  and  $\mathbf{X}_n$  are the fading matrix and the space-time codeword corresponding to node  $n$  and  $P_n$  is its interference power at RX, given by

$$P_n = \left(\frac{r_n}{R_n}\right)^b \left(\frac{S_n}{s_n}\right)$$

where  $R_n$  and  $S_n$  are the distance and shadowing, respectively, between node  $n$  and RX and  $r_n$  and  $s_n$  are the distance and shadowing between node  $n$  and its receiver. The term  $\frac{r_n^b}{s_n}$  reflects the PC applied by node  $n$  to its receiver.

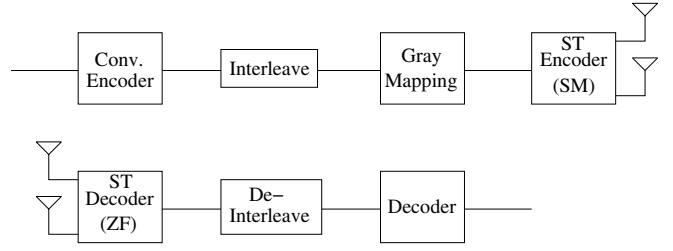


Fig. 1. TX and RX block diagrams. The terms in the parentheses correspond to SM mode.

Given  $\alpha_n$  and  $P_n$ , the matrix  $\mathbf{W} = \sum_n \alpha_n \sqrt{P_n} \mathbf{H}_n \mathbf{X}_n$  has entries  $w_{ij}$  which are independent random variables, with variance  $M_T \sum_n \alpha_n P_n$ . Assuming PSK modulation,  $w_{ij}$  are Gaussian, i.e.  $w_{ij} \sim \mathcal{CN}(0, M_T \sum_n \alpha_n P_n)$ . In the case of QAM modulation, the Gaussian assumption for  $w_{ij}$  is simply an approximation.

In the SM mode,  $m$  symbols, with  $m = 1, \dots, M_T$ , are concurrently transmitted from  $m$  antennas. This means that the rate of transmission is - at least -  $m$  times that of the STBC mode. Also, unlike the STBC mode, FH takes place every symbol slot. If  $\mathbf{x}$  is the transmitted vector, then the received vector  $\mathbf{y}$  is given by

$$\mathbf{y} = \mathbf{H}\mathbf{x} + \sum_n \alpha_n \sqrt{P_n} \mathbf{H}_n \mathbf{x}_n \quad (2)$$

where the definition of the different terms is the same as in (1), apart from  $\mathbf{x}_n$ , which is the vector transmitted by interferer  $n$ . Given  $\alpha_n$  and  $P_n$ , the interference vector  $\mathbf{w} = \sum_n \alpha_n \sqrt{P_n} \mathbf{H}_n \mathbf{x}_n$  has independent entries  $w_i \sim \mathcal{CN}(0, m \sum_n \alpha_n P_n)$ .

At the RX side, a ST decoder or a ZF detector processes  $\mathbf{Y}$  or  $\mathbf{y}$ , respectively. Let  $x_k$  represent a symbol at the output of the Gray mapper. For both modes of MIMO transmission, the equivalent channel model at the input of the de-interleaver/decoder is

$$y_k = \sqrt{a_k} x_k + w_k \quad (3)$$

where  $a_k$  is chi-squared distributed with parameter  $1/2$  and  $2N$  degrees of freedom,  $N$  denoting the spatial diversity order. Also, given  $\sigma_k^2 = q \sum_n \alpha_n P_n$ ,  $w_k \sim \mathcal{CN}(0, \sigma_k^2)$ , where  $q$  is the number of active TX antennas. For the STBC mode,  $N = M_T^2$  and  $q = M_T$ , while, for the SM mode,  $N = M_T - m + 1$  ( $m - 1$  antennas are used to suppress the self-interference by the other  $m - 1$  streams) and  $q = m$ .

### III. PERFORMANCE ANALYSIS

The decoder criterion for deciding that the codeword  $\hat{\mathbf{c}} = \{\hat{c}_k\}$  was sent is [9]

$$\hat{\mathbf{c}} = \arg \min_{\mathbf{c} \in \mathcal{C}} \left\{ \sum_{k=1}^{L_c} \min_{x \in \mathcal{X}_{c_k}^{i_k}} \frac{|y_k - \sqrt{a_k} x|^2}{\sigma_k^2} \right\}$$

where  $\mathcal{C}$  is the set of all transmitted codewords and  $\mathcal{X}_{c_k}^{i_k}$  denotes the set of constellation symbols that have bit  $c_k$  at position  $i_k = 1, \dots, l$ . The decoder is aware of the interleaving

strategy  $\{i_k\}$ , i.e. at which positions of the complex symbols the coded bits were mapped, as well as  $\{y_k, a_k, \sigma_k^2\}$ .

We now assume that the variables  $\{a_k, \sigma_k^2\}$  are *independent* within the span of the minimum distance error event of the code. This assumption is based on the interleaving of the bits within the codeword, as well as the fact that, due to hopping, it is likely that a different set of interferers is active in each symbol slot. The latter claim is experimentally justified in the appendix. Under the above criterion, the probability of the dominant error event is upper-bounded by [9], [10]

$$P_L = \frac{1}{\pi} \int_0^{\frac{\pi}{2}} \left[ \frac{1}{l2^l} \sum_{i=1}^l \sum_{c=0}^1 \sum_{x \in \mathcal{X}_c^i} \Phi \left( \frac{d_{x,x'}}{4 \sin^2 \theta} \right) \right]^L d\theta \quad (4)$$

where  $L$  is the Hamming distance,  $x'$  is the closest neighbor of  $x$  that has the complementary bit  $\bar{c}$  in position  $i$ ,  $d_{x,x'} = |x - x'|$  and  $\Phi(s)$  is the moment generating function of the random variable  $\frac{\alpha}{\sigma^2}$  (due to the assumption of independence across  $k$ , the subscript  $k$  has vanished). Given  $\sigma^2$ , it is well known that

$$\mathbb{E}_{\alpha|\sigma^2} \left[ e^{-\frac{\alpha}{\sigma^2} s} \right] = \left( 1 + \frac{s}{\sigma^2} \right)^{-N}$$

Hence, the evaluation of  $\Phi(s)$  and therefore  $P_L$  comes down to carrying out the expectation

$$\Phi(s) = \mathbb{E}_{\sigma^2} \left[ \left( 1 + \frac{s}{\sigma^2} \right)^{-N} \right] \quad (5)$$

for which the distribution of the interference power,  $\sigma^2$ , is required.

If each codeword has  $L_c$  bits, the packet success probability is approximated by  $P_s \simeq (1 - P_b)^{L_c}$ , where  $P_b$  is the bit error probability (BEP). Knowing  $P_L$ , the BEP can be coarsely approximated by

$$P_b \simeq \frac{w_L P_L}{b_c}$$

where  $w_L$  is the total information weight of all minimum distance error events and  $b_c$  is the number of information bits per trellis branch.

#### A. Distribution of the interference power

For both MIMO modes, the total interference power is

$$z = \sigma^2 = q \sum_n \alpha_n P_n = q \sum_n \alpha_n \beta_n R_n^{-b}$$

where  $\beta_n = \frac{r_n^b S_n}{s_n}$ . The authors in [3] proved that, for  $b > 2$ , the characteristic function of  $z$  is

$$\Phi_z(\omega) = \mathbb{E}[e^{i\omega z}] = \exp \left( -\pi \lambda_{\text{eff}} \Gamma \left( 1 - \frac{2}{b} \right) e^{-\frac{i\pi}{b}} \omega^{\frac{2}{b}} \right)$$

for  $\omega \geq 0$ , where  $\lambda_{\text{eff}} = \frac{\lambda p q^{\frac{2}{b}} \bar{\beta}}{M}$  is the *effective density*,  $\bar{\beta} = \mathbb{E}[\beta^{\frac{2}{b}}]$  and  $\Gamma(\cdot)$  denotes the gamma function. This is a special case of the characteristic function of *stable distributions* [11], [12], with stability parameter  $\alpha = \frac{2}{b}$  (the exponent of  $\omega$  in the expression of the characteristic function). The corresponding pdf can be obtained as an infinite series [3]. However, for the

practical case of ground propagation ( $b = 4$  or  $\alpha = 1/2$ ), the pdf has the closed form solution

$$f(z) = \frac{\pi}{2} \lambda_{\text{eff}} z^{-\frac{3}{2}} \exp \left( -\frac{\pi^3 \lambda_{\text{eff}}^2}{4z} \right), \quad z > 0 \quad (6)$$

where  $\lambda_{\text{eff}} = \frac{\lambda p \sqrt{q} \bar{\beta}}{M}$ . This is a special case of the Lévy distribution with scale parameter  $c = \frac{\pi^3 \lambda_{\text{eff}}^2}{2}$ . Since the first order moment of the Lévy distribution does not exist [12], the scale parameter  $c$  provides an indication of the spread of the interference power values. The ‘‘average’’ signal-to-interference ratio (SIR) is defined as  $\gamma = c^{-1/2}$ .

1) *The value of  $\bar{\beta}$* : Regarding the value of  $\bar{\beta}$ , we have

$$\bar{\beta} = \mathbb{E}[r^2] \mathbb{E} \left[ \left( \frac{S}{s} \right)^{\frac{2}{b}} \right]$$

Since  $\left( \frac{S}{s} \right)^{\frac{2}{b}}$  is lognormal with variance  $\frac{8\sigma_s^2}{b^2}$ ,

$$\mathbb{E} \left[ \left( \frac{S}{s} \right)^{\frac{2}{b}} \right] = \exp \left( \frac{4c_s^2 \sigma_s^2}{b^2} \right)$$

with  $c_s = \frac{\ln 10}{10}$ .

The value of  $\mathbb{E}[r^2]$  depends on the routing strategy. The statistics of the NFP and MFR neighbor are thus required. In the NFP case, the pdf of  $r$  - given that there is at least one node in the desired direction - is [2]

$$f_{\text{NFP}}(r) = \lambda \pi r e^{-\frac{\lambda \pi r^2}{2}}, \quad 0 < r \leq R_0$$

As a result

$$\mathbb{E}[r^2]_{\text{NFP}} = \lambda \pi \int_0^{R_0} r^3 e^{-\frac{\lambda \pi r^2}{2}} dr = \frac{2}{\lambda \pi} \gamma(2, N_0/2)$$

where  $\gamma(\alpha, x) = \int_0^x e^{-t} t^{\alpha-1} dt$ ,  $\alpha > 0$  is the incomplete gamma function and  $N_0 = \lambda \pi R_0^2$  is the average number of nodes within the range of the transmitter. Note that, for  $N_0 \rightarrow \infty$ ,  $\gamma(2, N_0/2) \rightarrow 1$  and  $\mathbb{E}[r^2]_{\text{NFP}} \rightarrow \frac{2}{\lambda \pi}$ .

The pdf of the MFR neighbor is also derived in [2]

$$f_{\text{MFR}}(r) = \int_{-\pi/2}^{\pi/2} \lambda r e^{-\lambda A(r, \theta)} d\theta, \quad 0 < r \leq R_0$$

with

$$A(r, \theta) = R_0^2 \cos^{-1} \left( \frac{r \cos \theta}{R_0} \right) - R_0 r \cos \theta \sqrt{1 - \left( \frac{r \cos \theta}{R_0} \right)^2}$$

We thus have

$$\begin{aligned} \mathbb{E}[r^2]_{\text{MFR}} &= \lambda \int_0^{R_0} r^3 dr \int_{-\pi/2}^{\pi/2} e^{-\lambda A(r, \theta)} d\theta \\ &= \frac{N_0^2}{\lambda \pi^2} \int_0^1 t^3 dt \int_{-\pi/2}^{\pi/2} e^{-\frac{N_0}{\pi} \tilde{A}(t, \theta)} d\theta \end{aligned}$$

where  $\tilde{A}(t, \theta) = \cos^{-1}(t \cos \theta) - t \cos \theta \sqrt{1 - (t \cos \theta)^2}$ .

### B. Evaluation of $P_L$

Using the closed form expression of the interference power pdf for  $b = 4$  in (5), we have

$$\begin{aligned}\Phi(s) &= \frac{\pi\lambda_{\text{eff}}}{2} \int_0^{+\infty} z^{-3/2} e^{-\frac{\pi^3\lambda_{\text{eff}}^2}{4z}} \left(1 + \frac{s}{z}\right)^{-N} dz \\ &= \frac{\pi\lambda_{\text{eff}}}{2} \int_0^{+\infty} z^{-1/2} e^{-\frac{\pi^3\lambda_{\text{eff}}^2 z}{4}} (1 + sz)^{-N} dz \\ &= \frac{\pi^{3/2}\lambda_{\text{eff}}}{2\sqrt{s}} \Psi\left(\frac{1}{2}, \frac{3}{2} - N; \frac{\pi^3\lambda_{\text{eff}}^2}{4s}\right)\end{aligned}\quad (7)$$

for  $s > 0$ , with

$$\Psi(a, b; x) = \frac{1}{\Gamma(a)} \int_0^{\infty} t^{a-1} (1+t)^{b-a-1} e^{-xt} dt, \quad a > 0$$

denoting the confluent hypergeometric function of the second kind (see [13], p.1085). Substituting (7) in (4),  $P_L$  is computed after carrying out the integration over  $\theta$ . In fig.2,  $P_L$  is plotted vs.  $\gamma$  for different values of  $L$  and  $N$  and BPSK modulation. We observe that, increasing the spatial diversity order  $N$  for a given  $L$ , only leads to a shift of the curve to the left, i.e. an increase in coding gain.

### C. No coding

In the case of no coding, decisions are made on the symbol level. The packet success probability is therefore given by  $P_s = (1 - P_e)^{\frac{L_c}{l}}$ , where  $P_e$  is the symbol error probability and  $\frac{L_c}{l}$  is the number of symbols in the packet. From p. 271-273 of [10], for  $M_P = 2^l$ -PSK, we have

$$P_e = \frac{1}{\pi} \int_0^{\frac{(M_P-1)\pi}{M_P}} \Phi\left(\frac{g_{\text{PSK}}}{\sin^2\theta}\right) d\theta \quad (8)$$

where  $g_{\text{PSK}} = \sin^2\frac{\pi}{M_P}$ . For  $M_Q = 2^l$ -QAM ( $l$  even)

$$\begin{aligned}P_e &= \frac{4}{\pi} \left(1 - \frac{1}{\sqrt{M_Q}}\right) \int_0^{\frac{\pi}{2}} \Phi\left(\frac{g_{\text{QAM}}}{\sin^2\theta}\right) d\theta \\ &\quad - \frac{4}{\pi} \left(1 - \frac{1}{\sqrt{M_Q}}\right)^2 \int_0^{\frac{\pi}{4}} \Phi\left(\frac{g_{\text{QAM}}}{\sin^2\theta}\right) d\theta\end{aligned}\quad (9)$$

with  $g_{\text{QAM}} = \frac{3}{2(M_Q-1)}$ .

## IV. INFORMATION EFFICIENCY

The rate at which a TX successfully transmits packets, or packet throughput,  $PT$ , is given by  $PT = \tau(p) \cdot P_s$ . The spectral efficiency,  $SE$ , is defined as

$$SE = \frac{R_c \cdot R_{ST} \cdot l \cdot PT}{M} = \frac{R_c \cdot R_{ST} \cdot l \cdot \tau(p) \cdot P_s}{M}$$

where  $R_c$  is the rate of the convolutional code,  $R_{ST}$  is the rate of the STBC or  $R_{ST} = m$  for the SM mode.

As first described in [1]-[3] and, more recently, in [4]-[7], in a multi-hop network it is not only  $PT$  or  $SE$  that matters but also how far a packet is transmitted in each hop. A small transmission range leads to higher throughput due to reduced levels of interference, however the number of hops that a packet must make to reach its final destination is increased.

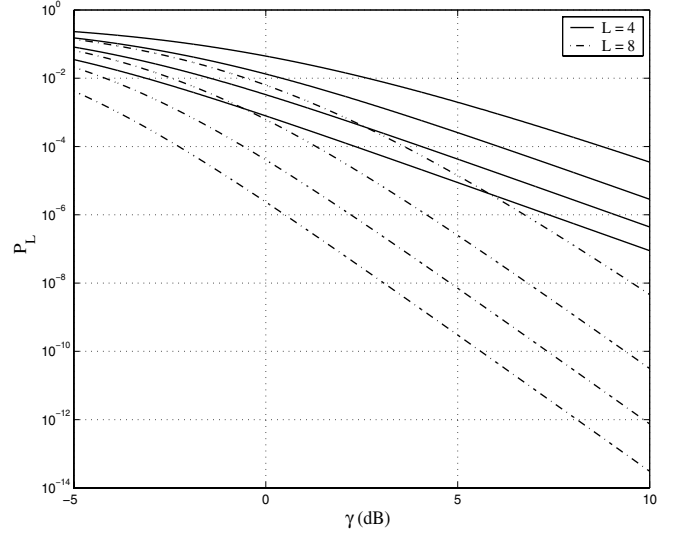


Fig. 2.  $P_L$  plotted vs.  $\gamma$  for Hamming distance  $L = 4, 8$  and spatial diversity order  $N = 1, 2, 4, 8$ .

The latter is a potential source of delay, as well as increased internal network traffic.

To this end, information efficiency,  $IE$ , is defined as

$$IE = SE \cdot E[r_f]$$

where  $E[r_f]$  is the expected forward progress that a packet makes towards its final destination, given the chosen routing strategy. If  $(r, \theta)$  is the location of the NFP or MFR neighbor, then,  $r_f = r \cos \theta$  and

$$E[r_f] = \int_{-\pi/2}^{\pi/2} \int_0^{R_0} r \cos \theta f(r, \theta) dr d\theta$$

For NFP routing, we have

$$\begin{aligned}E[r_f]_{\text{NFP}} &= \int_{-\pi/2}^{\pi/2} \int_0^{R_0} r \cos \theta \lambda r e^{-\frac{\lambda \pi r^2}{2}} dr d\theta \\ &= \frac{(2/\pi)^{3/2}}{\sqrt{\lambda}} \gamma(3/2, N_0/2)\end{aligned}$$

Similarly, for MFR routing we obtain

$$E[r_f]_{\text{MFR}} = \frac{(N_0/\pi)^{3/2}}{\sqrt{\lambda}} \int_0^1 t^2 dt \int_{-\pi/2}^{\pi/2} \cos \theta e^{-\frac{N_0}{\pi} \tilde{A}(t, \theta)} d\theta$$

## V. NUMERICAL RESULTS

The MIMO transmission modes shown in table I are considered. The last mode corresponds to SM with only two out of the available four antennas. We set  $M = 50$ ,  $L_c = 1000$ ,  $l = 2$  (QPSK) and  $\sigma_s = 8$ . For each value of  $N_0$ , the  $IE$  is - numerically - optimized over  $p$ . Furthermore, the  $IE$  is normalized by  $\sqrt{\lambda}$  so that the results do not depend on a specific node density.

In fig.3, the  $IE$  is plotted vs.  $N_0$  for the optimum  $R_c = 1/2$  convolutional code with  $L = 5$ . The solid lines correspond to MFR routing and the dash-dot lines to NFP. For NFP routing,

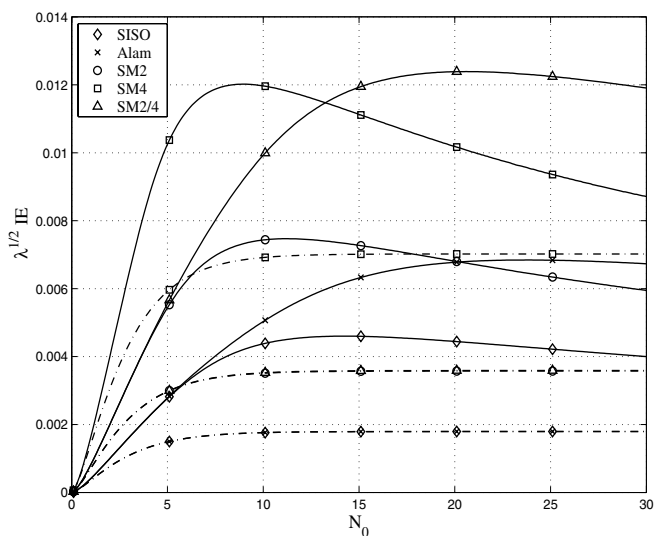


Fig. 3.  $\sqrt{\lambda}IE$  vs.  $N_0$  for the optimal rate-1/2 convolutional code with  $L = 5$ , NFP/MFR routing and different MIMO modes.

the SISO and Alam lines overlap, indicating that an increase in diversity order is unnecessary in terms of  $IE$ . The same holds for SM2 and SM2/4 which correspond to the same rate  $R_{ST} = 2$ , but  $N = 3 > 1$  for SM2/4. The highest  $IE$  for NFP is achieved by SM4. Note that the NFP lines are relatively constant for different  $N_0$ , which is attributed to the fact that the expected forward progress,  $E[r_f]$ , as well as the expected transmitted power to the RX,  $E[r^2]$ , are almost constant with increasing  $N_0$ . A similar result was noted in [2].

Regarding MFR routing, the trade-off between transmitting further and generating more interference is more apparent. SM2 outperforms Alam for all but the largest transmission ranges. This is not the case for SM4 and SM2/4; SM4 is preferable up to  $N_0 \approx 13$  because it achieves larger data rate, however the situation is reversed for  $N_0 > 13$ , as SM2/4 provides more error protection against the increasing interference that results from a larger transmission range.

A comparison between NFP and MFR reveals that all MIMO modes achieve higher  $IE$  with MFR than NFP routing. However, in fig.4, plotting the optimal  $p$  (the one that achieves the maximum  $IE$  for each  $N_0$ ) vs.  $N_0$ , it is apparent how sensitive the  $IE$  is to the choice of  $p$ , for MFR routing. As pointed out in [2], this can be a considerable disadvantage if the nodes have no way of knowing the optimum  $p$ . Also note that SM2 and SM4 correspond to the smallest transmission probabilities; the nodes can transmit more data but have to do

TABLE I  
MIMO TRANSMISSION MODES

Mode	$M_T$	$N$	$R_{ST}$	$q$
Single antenna (SISO)	1	1	1	1
Alamouti STBC (Alam)	2	4	1	2
SM 2x2 (SM2)	2	1	2	2
SM 4x4 (SM4)	4	1	4	4
SM 2x2 with 4 ant. (SM2/4)	4	3	2	2

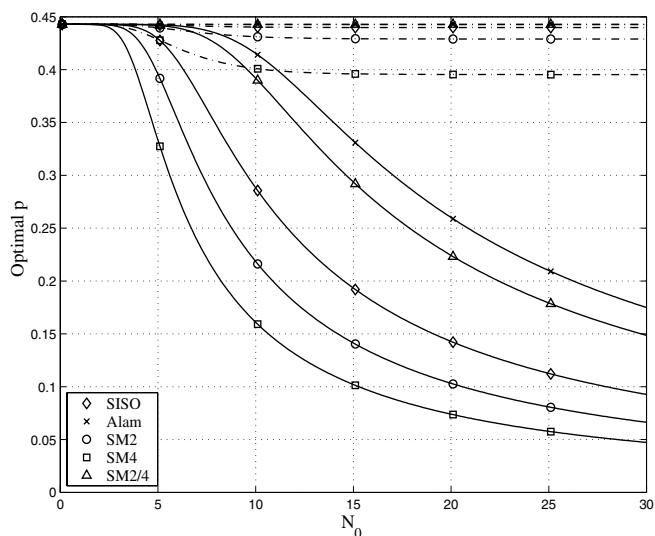


Fig. 4. Optimal  $p$  vs.  $N_0$  for the optimal rate-1/2 convolutional code with  $L = 5$ , NFP/MFR routing and different MIMO modes.

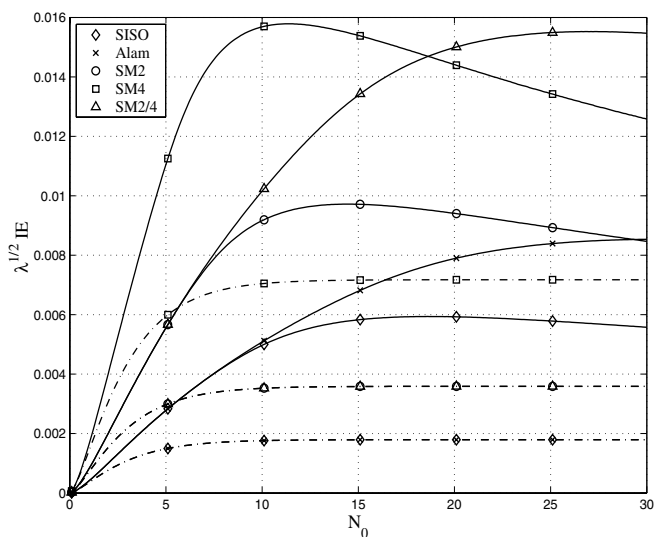


Fig. 5.  $\sqrt{\lambda}IE$  vs.  $N_0$  for the optimal rate-1/2 convolutional code with  $L = 8$ , NFP/MFR routing and different MIMO modes.

so less often to avoid creating excessive interference.

The above observations hold when the code diversity order is increased to  $L = 8$  (fig.5). However, the enhanced error protection allows the use of SM for larger transmission ranges, e.g. SM2 completely outperforms Alam for all  $N_0$ .

Finally, in fig.6, the  $IE$  is plotted for a system with no coding. It is apparent how the  $IE$  decreases with  $N_0$  for all modes combined with MFR routing, after having reached a maximum for very small  $N_0$ . NFP routing is thus more preferable when coding is not employed for error protection.

## VI. CONCLUDING REMARKS

We presented a performance analysis for an *ad hoc* network with FH-MIMO transceivers. Coding and its ability to harness the interference diversity is central to the evaluation

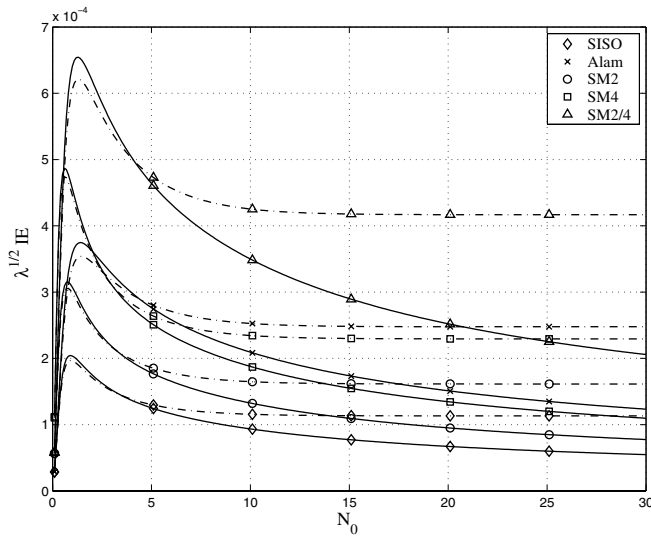


Fig. 6.  $\sqrt{\lambda}IE$  vs.  $N_0$  for no coding, NFP/MFR routing and different MIMO modes.

of the BER and network performance measures such as the information efficiency. MIMO techniques were also employed for further error protection and/or increase of the data rate.

For indicative values of the system parameters, we demonstrated that the choice of MIMO transmission depends strongly on the error correcting capability of the code and the routing strategy. It was also observed that, when there is no knowledge of the interference other than its power, increasing the spatial diversity order  $N$ , only enhances the coding gain in terms of BER vs.  $\gamma$ .

It is interesting to repeat the analysis for a more general interference power distribution than (6), which could be the result of a propagation exponent other than  $b = 4$  or the existence of scheduling in the network, that inhibits the presence of interferers too close to the RX. Exploring the effect of the presented FH-MIMO physical layer on network metrics other than the  $IE$  is also a topic of future work.

#### APPENDIX

The following experiment was carried out. The RX was placed in the center of a disc with an area five times the transmission range. For  $N_0 = 10$ , a realization of the Poisson random process was generated and the total interference power computed over 1000 slots, where, in each slot, each interferer was active with probability  $1/M$  and its power was unity. The normalized autocorrelation of the interference power was then computed over time. The experiment was repeated and the normalized autocorrelation averaged over 100 different realizations of the Poisson process. The results are presented in fig.7. As the number of frequencies is increased, the correlation drops significantly and for  $M = 50$  or  $M = 100$  takes very small values. The effect of these finite correlation values on the performance can be evaluated via simulation.

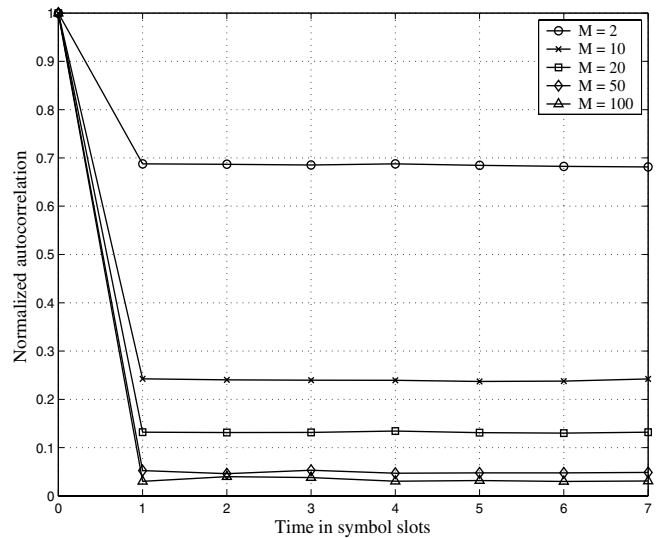


Fig. 7. Normalized interference autocorrelation vs. time in symbol slots for different values of  $M$ . The propagation constant is  $b = 4$ .

#### REFERENCES

- [1] H. Takagi and L. Kleinrock, "Optimal transmission ranges for randomly distributed packet radio terminals," *IEEE Trans. Commun.*, vol. 32, pp. 246–256, Mar. 1984.
- [2] T.-C. Hou and V. O. K. Li, "Transmission range control in multihop packet radio networks," *IEEE Trans. Commun.*, vol. 34, pp. 38–44, Jan. 1986.
- [3] E. S. Sousa and J. A. Silvester, "Optimum transmission ranges in a direct-sequence spread-spectrum multihop packet radio network," vol. 8, pp. 762–771, June 1990.
- [4] M. W. Subbarao and B. L. Hughes, "Optimal transmission ranges and code rates for frequency-hop packet radio networks," *IEEE Trans. Commun.*, vol. 4, pp. 670–678, Apr. 2000.
- [5] M. R. Souryal, B. R. Vojcic, and R. L. Pickholtz, "Information efficiency of multihop packet radio networks with channel-adaptive routing," vol. 23, pp. 40–50, Jan. 2005.
- [6] —, "Adaptive modulation in ad hoc DS/CDMA packet radio networks," *IEEE Trans. Commun.*, vol. 54, pp. 714–725, Apr. 2006.
- [7] S. P. Weber, X. Yang, J. G. Andrews, and G. de Veciana, "Transmission capacity of wireless ad hoc networks with outage constraints," *IEEE Trans. Inform. Theory*, vol. 51, pp. 4091–4102, Dec. 2005.
- [8] H. Sui and J. R. Zeidler, "Information efficiency and transmission range optimization for coded MIMO FH-CDMA ad hoc networks in time-varying environment," 2007, *submitted to the IEEE Trans. on Comm.*
- [9] G. Caire, G. Taricco, and E. Biglieri, "Bit-interleaved coded modulation," *IEEE Trans. Inform. Theory*, vol. 44, pp. 927–946, May 1998.
- [10] M. K. Simon and M.-S. Alouini, *Digital Communication over Fading channels, a unified approach to performance analysis*, 1st ed. Wiley Series in Communications and Signal Processing, 2000.
- [11] J. Nolan, "An introduction to stable distributions," 2005, url: <http://academic2.american.edu/~jpnolan/stable/stable.html>.
- [12] M. Shao and C. L. Nikias, "Signal processing with fractional lower order moments: stable processes and their applications," *Proc. IEEE*, vol. 81, pp. 986–1010, July 1993.
- [13] I. S. Gradshteyn and I. M. Ryzhik, *Table of integrals, series and products*, 4th ed. Academic Press, 1994.